Image-processing assisted characterization of spray injection systems

Image-processing assisted characterization of spray injection systems

E. Baccaglini, M. Gavelli, M. Morello, N. Raimondo, R. Scopigno
Istituto Superiore Mario Boella, Via P.C. Boggio, 61, 10136 Torino (Italy)
Email: baccaglini@ismb.it

***Abstract*—The objective of this work is to investigate the spray characteristics of a fuel injection nozzle. The analysis is performed by means of a framework which exploits different image processing techniques to provide spray-related data to the operator. Innovative metrics are introduced to increase the accuracy and efficiency of the scheme. Experimental results show that it is possible to automatically get useful information about the spray distribution, asymmetries and key properties together with the capability to measure significant angles and other information to detect anomalies in the injection system.**

I. Introduction

Automatic spray characterization by means of image processing can be of great benefit in the field of automotive. The selection of a particular injector for a given application strongly depends on many parameters i.e. the mean drop diameter, the mass distribution, the jet speed. The precise characterization of sprays is a challenging task and a very specialized area of measurement [1]. One of the main reasons is the fact that the injection of the fuel in an engine is a transient event (usually of a few milliseconds of duration) and thus it requires the adoption of high frame-rate cameras for the acquisition step. Furthermore, some measurements such as the spray-tip penetration involve macroscopic parameters while others require the study of microscopic characteristics.

Nowadays, the fuel spray obtained from a port fuel injector (PFI) is the most common type in the automotive industry [2]. In PFI engine there is a relatively long time frame available for mixture generation outside the cylinder and the dynamic conditions are easier to control with respect to other injection systems (e.g. direct injection). Injecting the fuel into the intake manifold continuously or sequentially allows for long trajectories of fuel droplets. The spray is usually injected in the combustion chamber at low-pressure in a time frame which usually lasts from 2 to 15 ms. Newer gasoline direct injector (GDI) produces a fine spray over a 0.5 to 5.0 ms time injection. Furthermore, the pressure in this injector is much higher. GDI systems differ from traditional PFI systems in that the fuel is injected directly into the cylinder rather than into the intake ports prior to the intake valves. This allows to achieve more flexibility over the conditions and the mixture within the cylinder, and thus the designer can control the output emissions to a much higher degree. The spray characteristics strongly influence the vaporization process and hence these characteristics are of paramount importance to guarantee combustion efficiency and control of engine-out emissions. Many manufacturers have developed multi-hole nozzles [3] for GDI applications. These injectors are similar to Diesel injectors and they can deliver fuel through several holes, although the conical pattern is much narrower than the ones in Diesel applications. The main advantage of the multi-hole injector is that many different spatial distributions of fuel mass can be obtained by varying the hole geometry. These injectors lead to new challenging image processing issues e.g. the correct evaluation of the number of spray (because some of them may be hidden by others) or the evaluation of the opening angle for each jet. For this type of injectors, the knowledge of where exactly this fuel should be targeted is not likely to be known during engine development, so some trial and error experiments usually take place in developing the optimized nozzle tip. Image processing techniques can thus be of great benefits to better analyze these injectors.

In [4], the effects of injection pressure, ambient pressure and ambient temperature are examined using high speed CCD cameras for GDI. Image processing is performed with MatLab and the analysis encompasses the spray tip penetration and the spray cone angle. In [5], image processing is applied to extract macroscopic and microscopic attributes including spray pattern, spray-cone angle, spray tip penetration and velocity, particle size distribution, and particle velocity. Image processing is applied over images captured using laser technology. The effects of changing in fuel-pressure, injector frequency and nozzle size are discussed as well. A similar work was presented in [6] for the analysis and characterization of a Delphi diesel common rail fuel injection system. In [7], authors experimentally evaluate the injection pressure impact on spray characteristics for pressures reaching 250 MPa. In [8] the analysis of the mixture formation in a slightly lean burn GDI engine is performed by using experimental and numerical techniques. Authors propose an architecture based on UV visible natural emission digital imaging in the optically accessible combustion chamber by means of a single camera. In [9] authors investigate the structure of a gasoline spray from a GDI injector with a X-ray tomography and where the GDI injector is inserted in a high-pressure rotating device. Although the spray characteristics of an injection system can be usually better described using two or more cameras or laser systems, the authors of some recent works [10], [11], [12] prefer to adopt a single camera to perform this task to significantly reduce the cost of the system. It is worth noting that the SAE J2715 document [1] has been recently developed by the SAE Gasoline Fuel Injection Standard Committee and addresses the subject of characterizing automotive gasoline fuel sprays. The recommended practices apply to the sprays that are used both in PFI and GDI engine applications and its objective is to promote uniformity in the field of spray characterization throughout the automotive industry.

978-1-4799-7800-7/15/$31.00 ©2015 IEEE

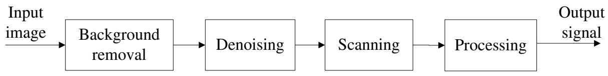

Fig. 1. Block diagram of the proposed framework.

In this paper we propose an effective low-cost image-processing based system able to automatically investigate the spray characteristics of a fuel injection nozzle by means of a single camera. The framework has been tested for gasoline engines and can be generalized to support compression ignition engines (i.e. Diesel engines). We adopted both traditional and innovative metrics to test the effectiveness of the proposed approach and both single and multi-hole injectors are considered to validate the proposed approach. In addition to the standard metrics proposed by SAE, the system also evaluates the jet variance and the spray histogram. Furthermore, a graphical user interface allows to control all the free parameters of the system and gives the opportunity to the operator to draw an ideal mask the spray should adhere to. The rest of the paper is organized as follows. In Sec. II, we describe the proposed algorithm while in Sec. III we discuss some experimental results. The graphical user interface is described in Sec. IV and conclusions and future developments are given in Sec. V.

II. Proposed approach

The proposed architecture encompasses four main processing steps once the spray has been successfully captured by a suitable high frame-rate camera (e.g. a CCD camera @ $20k$ fps). As shown in Fig.1, the steps performed in the proposed framework are:

1) image background removal,
2) image denoising,
3) image scanning,
4) data processing.

The output of the algorithm is a signal which informs the operator whether the spray is compliant with a predefined set of acceptable values of spray characteristics.

As a first step, once the image has been acquired, a background removal routine is applied to improve the image characteristics. This task is usually performed by comparing a pre-loaded background image with the acquired image. The difference between the two images allows to extract the cone pattern. The reference background image can be periodically updated before the fuel is injected in order to correctly compensate illumination variations.

The denoising stage includes a median filter (or more sophisticated techniques) which removes salt-and-pepper noise which may arise from the background removal stage but also from unexpected image degradation in the preprocessing stages. The denoising step is crucial to avoid that some pixels are wrongly associated to the spray jet. This stage is followed by the computation of both the histogram and the probabilities of each intensity level to successfully perform the Otsu's method [13] to convert the gray-level image to a binary image containing only the spray.

Then, the (binary) image scanning step allows to map the image into a bi-dimensional array which will be further processed. The proposed approach scans the image with respect to the distance ρ from the nozzle and the angle θ. The algorithm scans the area of the spray with a radius of variable length ρ (depth) and at each step stores in a matrix the number of pixels that fall on the correspondent segment. This procedure is iterated for each angle θ in the range [θ_{max}, θ_{min}] and each ρ. In the example shown in Fig.2, starting with the segment CD, the algorithm scans the image up to segment CE with a radius of variable length. The range [θ_{max}, θ_{min}] and the granularity of θ and ρ are user-defined parameters.

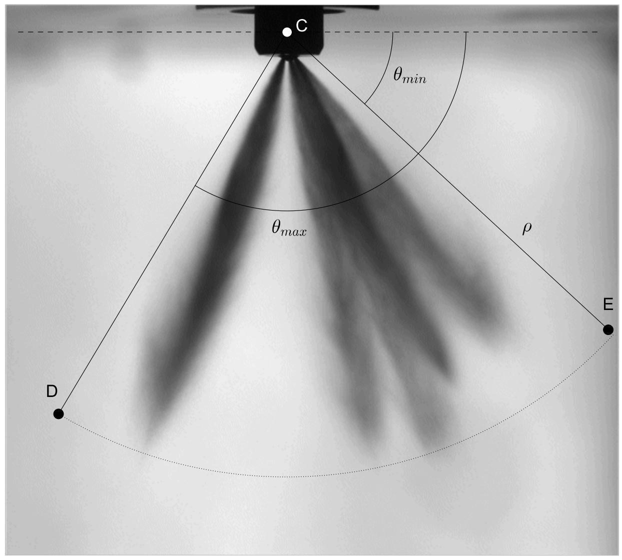

Fig. 2. An example of a GDI jet at 100 bar with the definition of radius ρ and the θ angles.

After storing the number of pixels corresponding to the spray collected as a function of the angle θ and ρ, the output matrix can be indexed as (ρ, θ) = (row, column).

Once this stage is completed, the data processing algorithm extracts from the matrix some parameters which have been considered relevant by SAE J2715 [1] as shown in Fig.3 and other new metrics and features to inform the operator about possible mismatches with respect to the expected values. The proposed algorithm can extract:

1) spray tip penetration PX
2) spray bend angle θ_B
3) opening angles θ_L and θ_R with respect to the spray axis and the injector axis
4) near- and far- field angle θ_N, θ_F
5) jet variance wrt the spray axis σ_s and the injector axis σ_i
6) distance of the scanned image from an ideal model
7) image histogram

The first four metrics represent the state-of-the-art to evaluate the spray efficiency while the others are new. The *spray tip penetration* PX is often adopted in literature [1] to describe the efficiency of the jet injector. It is defined as the maximum distance of the jet from the nozzle and it is a function of the instant of time in which the image was taken. This value can be normalized with the nozzle diameter. The importance of this

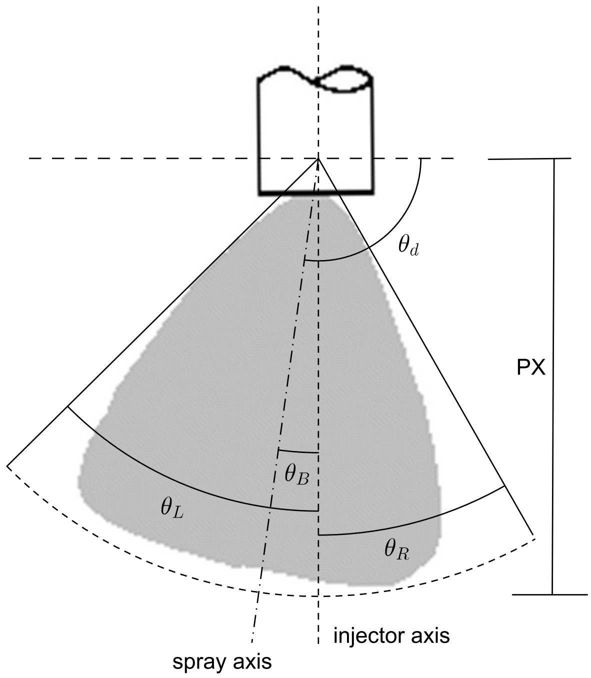

Fig. 3. Definition of some significant parameters processed by the proposed framework.

parameter is related to the fact that it is possible to deduce the jet speed and thus deduce whether the spray is flowing properly in the combustion chamber.

Usually, the angle between the spray axis and the injector axis is defined as *bend angle* (θ_B in Fig.3). If this value is too big, probably the injector is not working properly. This parameter allows to describe the *dominant direction* (also called spray axis) which represents the result of the weighted average of pixels with respect to the density of the spray. Some jets flow perpendicular to the nozzle while other can bend toward a precise direction. For implementation purposes, we adopt the variable θ_d to define the angle between this direction and the perpendicular to the injector axis (see Fig.3):

$$\theta_d = \frac{\int \theta\delta(\theta)d\theta}{\int \delta(\theta)d\theta}$$

In the above expression, the function $\delta(\theta)$ maps an angle θ to the number of pixels (belonging to the spray) that fall on the correspondent segment and the denominator represents the total number of spray pixels which normalizes the integral above. Once this integral has been evaluated, it is thus possible to deduce θ_B as $\theta_d - 90^\circ$ which may be more significant for the operator.

The proposed algorithm also reports the *opening angles* with respect to the injector axis (θ_L, θ_R) and the spray axis ($\theta_L - \theta_B$, $\theta_R + \theta_B$). Referring to Fig.3, these parameters define the left and right angles between the spray (or injector) axis and the maximum (minimum) value of θ which contains significant values. The analysis of these angles allows to estimate the asymmetry of the spray with respect to the dominant direction.

Other significant parameters as described in [5]-[14] are the *near-* and *far- field angles* (θ_N and θ_F). The near-field angle θ_N is defined as the angle between the tangents to the spray envelope at a distance 60 times greater than the nozzle diameter while θ_F is calculated at a distance 100 times greater. Both parameters allow to characterize how the spray spreads in the combustion chamber e.g. they can allow to deduce whether the spray produces a vortex effect or it flows straight toward the bottom of the combustion chamber.

An innovative parameter evaluated by the proposed approach is the *jet variance* defined as:

$$\sigma_s = \sqrt{\frac{\int (\theta - \theta_d)^2\delta(\theta)d\theta}{\int \delta(\theta)d\theta}}$$

When σ_s is low, the spray is dense around the spray axis. A similar metric, σ_i, is evaluated with respect to the injector axis.

The proposed algorithm can also automatically check whether the *distance* between the scanned image and an ideal model is within a range of acceptability. This parameter is a novelty with respect to previous works and allows to understand how the spray fits inside a particular mask and is thus compliant with a desired behavior. The ways the spray spreads can vary from an injector to an other and also within the same series of injectors. This parameter thus quickly allows the operator to understand whether a spray is standard-complaint within a tolerance range or not. The distance between an ideal reference model and the one obtained from the analysis of a jet can be expressed as the Euclidean distance in $\mathbf{R}^n$, as a weighted average or other metrics. The operators can tune this parameter offline providing the algorithm with a set of correct masks. These masks can be narrow or wide with respect to some particular critical angles. It is in fact possible to specify a range of acceptability for some particular angles which may be more relevant than others.

Finally, as a further and innovative feature implemented to characterize the spray as a whole, the *image histogram* evaluation is performed over the scanned jet. The histogram is available to the operator after the denoising filter and before the conversion to binary image. The plot of this function can provide extra information in the case the nozzle is partially broken or a jet is missing for a multi-hole injector. In fact, the count of pixels can rise a warning concerning an inefficiency of the spray, then the histogram can confirm this warning and rise an error to the operator. The histogram can be also adopted to automatically understand whether the mixture is not burning properly and/or it contains unwanted particles. Furthermore, it is possible to save the histogram of each scanned jet in order to build a database of injectors and spray for offline processing and data comparison.

III. Experimental results

The proposed architecture has been implemented in OpenCV and the whole project has been compiled as a library compatible with any .NET framework. In the following we describe some results obtained from the algorithm applied on the GDI jets of Fig.4 acquired with a resolution of 720×480 pixels. Sprays $A1$ and $A2$ refer to the same injector at different time frames while B and C refer to different injectors. As can be seen, the four samples represent a good subset to test the

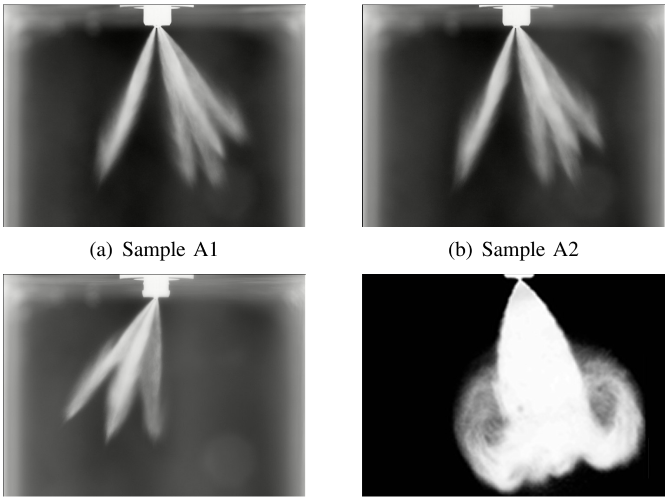

(a) Sample A1 (b) Sample A2

(c) Sample B (d) Sample C

Fig. 4. Some acquired sprays adopted for testing. Sprays $A1$ and $A2$ refer to the same injector at different time frames; B and C refer to different injectors.

TABLE I. RESULTS OF THE PROCESSING ALGORITHM OVER THE SAMPLES OF 4.

	sample A1	sample A2	sample B	sample C
PX	382	369	347	497
θ_B	-9.7	-8.9	16.4	-9.5
θ_L	26.5	27.0	42.0	22.5
θ_R	40.5	40.0	12.5	43.0
$\sigma_s(L;R)$	25.8; 16.6	25.2; 16.6	13.7; 14.6	11.8; 22.9
$\sigma_i(L;R)$	18.8; 24.3	19.2; 23.4	23.4; 6.5	17.1; 17.8
θ_N	66.5	67.0	54.0	57.0
θ_F	66.5	67.0	54.5	65.6

algorithms against. In fact, $A1$ and $A2$ are similar but not identical. It might be difficult even for an skilled operator to perceive the differences without the support of a computer-assisted tool. Sample B and C are taken from a different injector and they allow to better understand the benefits of the proposed metrics.

In Tab.I we summarize the evaluated parameters for all the jets of Fig.4. As it can be seen from the table, the process allows to describe in a very detailed manner each jet. The penetration index allows to gather information about spray formation. Sample $A1$ has a slightly higher PX with respect to $A2$ and this information would be hardly detected without an automatic image-processing based algorithm. The bend angle θ_B allows to describe how the jet is evolving in the combustion chamber. Negative values of θ_B mean that the spray is flowing mainly toward the right of the vertical. As an example, sample B tends to the left of the chamber ($\theta_B = 16.4°$) while the others tend to the left. Focusing on the injector A, the difference of approximately 1° (9.7° vs 8.9°) may be not negligible and may be due to an inefficiency of the injection system. The opening angles θ_L and θ_R are also significant to describe the way the jet spreads. In fact, all the proposed spray are asymmetric and the angles are very different one another. A further insight on the spray characteristics is given by the evaluation of the variances. Spray B is symmetric wrt the spray axis and then σ_s assumes nearly the same values for the left (L) and right (R) distribution (approximately 14°). Sample A is very different from B and C and the presence

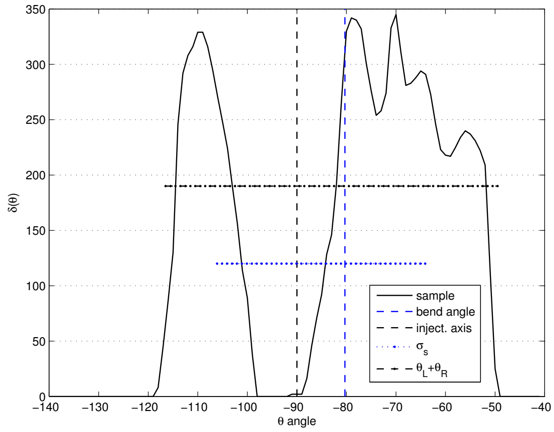

Fig. 5. Pixel distribution as a function of θ angle for the sample $A1$. Bend angle, injector axes, variances and opening angles are also reported.

of an isolated jet is highlighted by a high value for the left variance (approx 25°). Finally, the near- and far- field angles allow to detect curly spray as it can be seen for sample C. The value of θ_N (57.0°) significantly differs from the value of θ_F (65.6°) and this means that the spray expands in the chamber while flowing while for spray A, B and C these values are almost the same.

We report in Fig.5 a more detailed analysis of the sample $A1$. The figure reports the number of pixels $\delta(\theta)$ vs the θ angle for a given value of the ρ parameter. On the x-axes we report the θ angle in the range $[-140°; -40°]$ considering as 0° reference the perpendicular to the spray axis with anticlock wise positive angle orientation for implementation purposes. Analyzing the curve corresponding to the sample, it is possible to detect five different spray edges. The one to the left of the vertical corresponds to the angle in the range $[-115°; -95°]$ and the four edges placed to the right of vertical line have peaks around the values of $\{-78°, -70°, -65°, -55°\}$. The spray asymmetry is evident and the automatic processing performed over the matrix can detect it. Compared to a homogeneous vertical distribution across the vertical line corresponding to the angle of $-90°$, the right side of the spray contains a significant part of fuel. This feature can be extracted by evaluating and comparing the areas of the curve in the ranges $[-140°; -90°)$ and $(-90°; -40°]$. An asymmetry in the fuel distribution may be or may be not be desirable and an asymmetry can be accepted whether it is below a critical threshold. The figure also reports some significant parameters e.g. the bend angle (9.7° wrt to the vertical), the left and right jet variances with respect to the spray axis and the opening angles with respect to the injector axis.

Concerning the distance between the scanned image and an ideal model, in Fig.6 we report the analysis of sample $A1$ compared to sample $A2$ adopted as reference during the tests. Here, we adopt the sum of absolute differences to evaluate the distance between the two jets. Once the distance between the sample and the reference image has been calculated, it is possible to quantify how well a spray fits the model. As can be seen from the upper plot of the figure, the left side of the jet appears to be very similar to the model (the scanned image

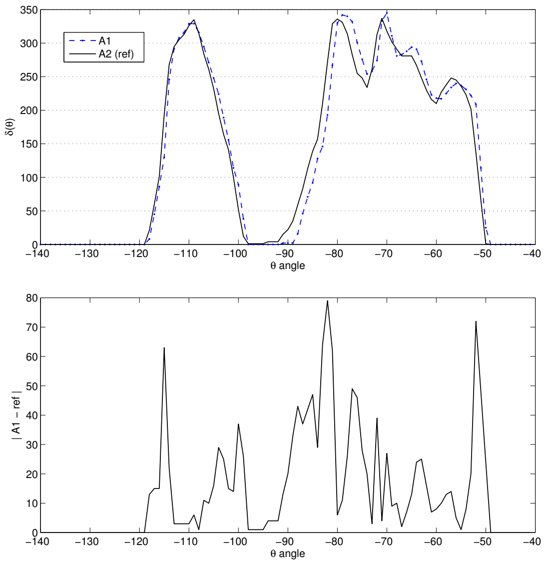

Fig. 6. Pixel distribution (above) and Euclidean distance (below) between the sample $A1$ and $A2$ (reference model).

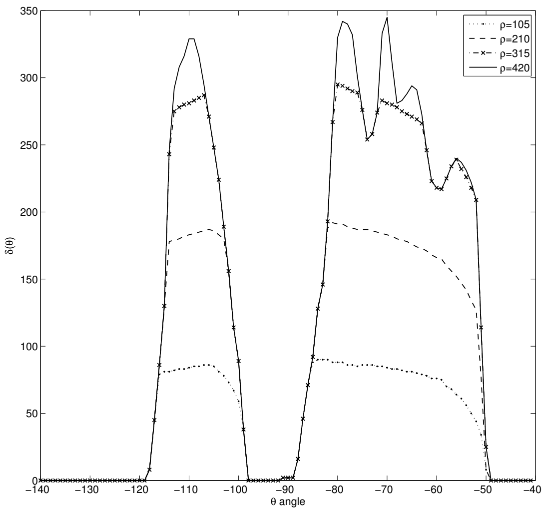

Fig. 7. Pixel distribution for sample $A1$ as a function of ρ and θ.

almost overlaps to the mask) while a bigger deviation can be appreciated for the right part of the flow. The lower plot of the figure shows the absolute difference between the reference and the scanned image for each angle θ. The difference can be as large as 80 pixels and this represents approximately the 20% of the spray tip penetration. This output can then raise an alarm signal because further investigation from the operator may be required. Automatic detection of this behavior can be of great benefit for injector analysis. Manual detection on the other side can be more expensive and less accurate and then should be performed only when strictly needed.

The proposed algorithm also allows to perform a pixel distribution analysis as a function of the segment ρ. Given a value of ρ, the algorithm outputs the variance and the dominant direction of the sub-portion of the stream for the selected ρ. This is particular useful in the case of curly and asymmetric jets and can provide significant information about the distribution and penetration of the spray at the time the picture was taken. In fact, as Fig.7 shows, if the spray analysis is performed with a low ρ, then only the region close to the nozzle is analyzed. It is then possible to detect two main jets around $-110°$ and around $-70°$. Increasing the value of ρ it is possible to understand that only when ρ is high enough (approx 300 px) the different jets are separated so no curly effect is detected. This operation can be performed automatically by the algorithm which can output a signal when a curly effect is detected merging this analysis with the near- and far- field values.

IV. Graphical User Interface

The proposed algorithm can be tuned with user-defined parameters to better adapt the application to the testing scenarios. All the customizable parameters can be set by means of a graphical user interface to allow the operator to control the system. The implemented interface includes the controls to:

- load a reference (model) image in the system to allow the comparison with a real scanned image;
- load the real scanned image;
- set the ranges of θ and ρ;
- define the metric to evaluate the distance between a reference image and a scanned one. At present, the operator can choose between the distance in $\mathbf{R}^2$ or a weighted distance in $\mathbf{R}^n$;
- define thresholds and boundaries (on penetration, opening angles...) so that the algorithm outputs a negative value in case some features of the spray do not match the ideal case within a given tolerance.

Fig.8 shows an example of the graphical user interface. On the top left the selected spray is shown together with some processed values overlay (e.g. opening angles, variances…). On the bottom left, the profile (central curve, in red) of the selected spray is showed inside the ideal mask (the upper blue curve represents the upper bound, the lower green curve represents the lower bound). In the central part of the GUI, the interface allows to tune the different parameters while on the right section of the window the algorithm reports the results. As can be seen, in the example all the processed parameters successfully passed the test except for the compliancy with the lower bounds of the ideal mask (marked as failed). Other windows allow the operator to load the reference model, adjust the range of acceptability for the ideal mask and store the spray histogram.

V. Conclusions

In this work we presented an innovative framework to process image obtain from scanning a fuel injection system. The system encompasses different stages to extract many spray characteristics. The experimental results show that high accuracy can be reached when both state-of-the-art and innovative metrics are adopted in the scheme. Further work will include

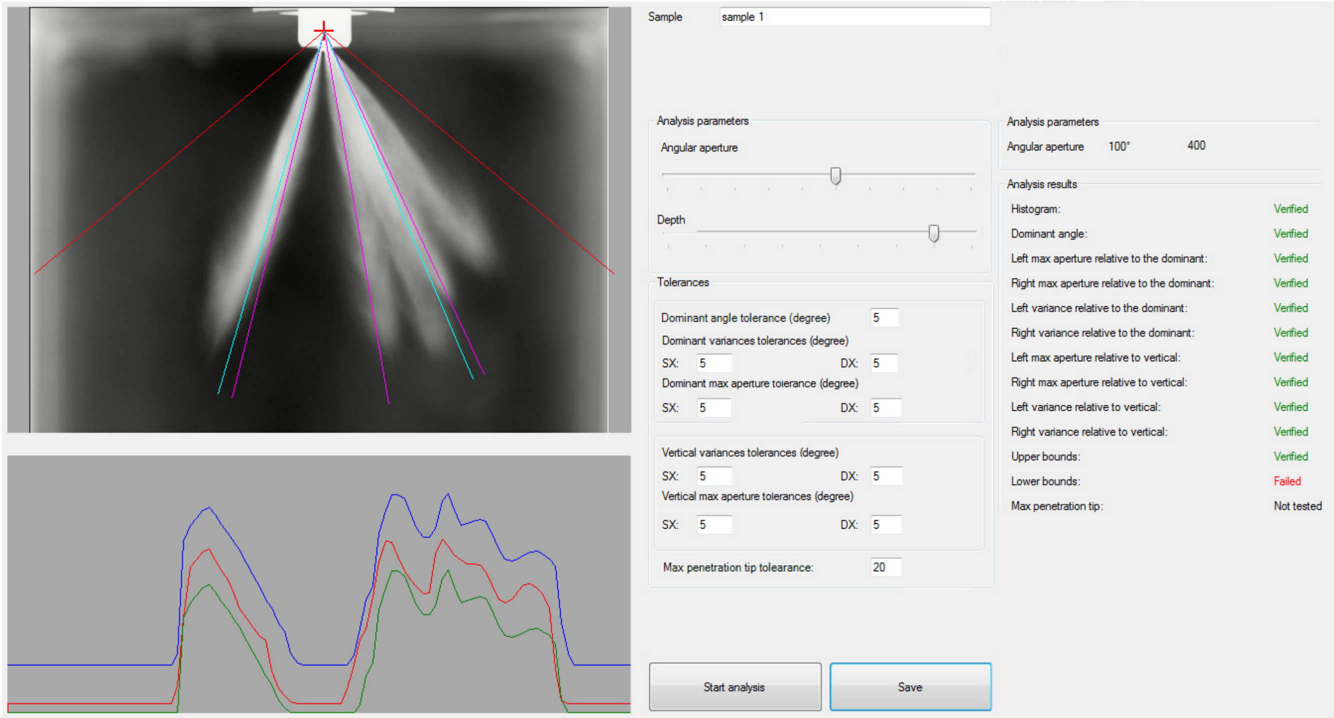

Fig. 8. The graphical user interface of the proposed framework includes the spray visualization (top left), the ideal mask visualization (bottom left), the set of tunable threshold (center) together with the analysis results (right).

the capabilities of dealing with multiple images to study the jet speed in the combustion chamber and the possibility to detect spray leaks in the nozzle. Multi-hole analysis is under research activity and will be performed with multiple cameras to detect hidden jets. Other key parameters are currently under investigation e.g. the image analysis using customizable opening angles and the spray impurity inspection by means of the image histogram analysis. Furthermore, other significant parameters e.g. the average spray-tip velocity and the average fuel area density will be addressed by means of multiple subsequent spray images.

REFERENCES

[1] D. Hung, D. Harrington, A. Gandhi, L. Markle, S. E. Parrish, J. S. Shakal, H. Sayar, S. D. Cummings, and J. L. Kramer, "Gasoline fuel injector spray measurement and characterization–a new SAE J2715 recommended practice," *SAE Int. J. Fuels Lubr*, vol. 1, no. 1, pp. 534–548, 2009.

[2] SAE Gasoline Fuel Injection Standards Committee and others, "Low pressure gasoline fuel injector," *SAE J1832, February*, 2001.

[3] F. Zhou, D. Harrington, and M. C. Lai, "Automotive gasoline direct injection engines," *SAE-R-315*, 2002.

[4] H. Ding, D. Huang, R. Huang, and Z. Wang, "Experiment study on spray structure of a multi-hole GDI injector," in *Electric Information and Control Engineering, 2011 International Conference on*. IEEE, 2011, pp. 5901–5904.

[5] R. Zakaria, P. Bryanston-Cross, and S. Addy, "Optical diagnostics in high-speed fuel spray; methodology and analysis," in *Photonics (ICP), 2010 International Conference on*. IEEE, 2010, pp. 1–6.

[6] J. Shao and Y. Yan, "Digital imaging based measurement of diesel spray characteristics," *Instrumentation and Measurement, IEEE Transactions on*, vol. 57, no. 9, pp. 2067–2073, 2008.

[7] E. Delacourt, B. Desmet, and B. Besson, "Characterisation of very high pressure diesel sprays using digital imaging techniques," *Fuel*, vol. 84, no. 7-8, pp. 859 – 867, 2005.

[8] M. Costa, L. Marchitto, S. Merola, and U. Sorge, "Study of mixture formation and early flame development in a research gdi (gasoline direct injection) engine through numerical simulation and uv-digital imaging," *Energy*, 2014.

[9] L. Allocca, S. Dabagov, D. Hampai, L. Marchitto, and S. Alfuso, "Tomography of a gdi spray by polyco based x-ray technique," SAE Technical Paper, Tech. Rep., 2013.

[10] S. Lee and S. Park, "Spray atomization characteristics of a GDI injector equipped with a group-hole nozzle," *Fuel*, vol. 137, pp. 50–59, 2014.

[11] M. A. Shost, M.-C. Lai, B. Befrui, P. Spiekermann, and D. L. Varble, "GDI nozzle parameter studies using LES and spray imaging methods," SAE Technical Paper, Tech. Rep., 2014.

[12] G. Hoffmann, B. Befrui, A. Berndorfer, W. F. Piock, and D. L. Varble, "Fuel system pressure increase for enhanced performance of GDI multi-hole injection systems," SAE Technical Paper, Tech. Rep., 2014.

[13] N. Otsu, "A threshold selection method from gray-level histograms," *Automatica*, vol. 11, no. 285-296, pp. 23–27, 1975.

[14] A. H. Lefebvre, *Atomization and sprays*. CRC Press, 1989, vol. 1040.